UDC 532.517 **DOI: 10.20998/2222-0631.2025.01(8).03**

V. A. VOSKOBOINICK, O. A. VOSKOBOINYK, A. V. VOSKOBIINYK, A. G. KHARCHENKO, D. V. TRUDENKO

FEATURES OF WAVE TRANSFORMATION BY A PERMEABLE BREAKWATER

The influence of the permeability of a breakwater on the wave transformation is studied. It is assumed that the vertical breakwater, in contrast to an absolutely rigid one, is characterized by a finite permeability and can absorb the energy of incoming incident waves. In this regard, the propagation of surface gravity waves in a rectangular coordinate system is investigated. Traditional realized examples of wave energy selection and their mathematical analysis are given. From the law of conservation of energy upon reflection from vertical walls follows the dependence for the reflection coefficient as a function of the transmission coefficient. The results of experimental studies of the propagation of surface gravity waves and their interaction with absorbing walls are presented. The dependences of the coefficients of reflection and transmission of the wave, as well as the coefficients of dissipation of wave energy depending on the permeability of the vertical wall, the depth of the flow, and the length of the incident wave are obtained. The integral and spectral characteristics of the wave field and pressure fluctuations on the streamlined surface of a permeable breakwater are presented.

Key words: wave transformation, permeable breakwater, numerical and physical simulation, wave reflection and transmission, wave energy dissipation.

В. А. ВОСКОБІЙНИК, О. А. ВОСКОБОЙНИК, А. В. ВОСКОБІЙНИК, А. Г. ХАРЧЕНКО, Д. В. ТРУДЕНКО

ОСОБЛИВОСТІ ТРАНСФОРМАЦІЇ ХВИЛЬ ПРОНИКНИМ ХВИЛЕЛОМОМ

Досліджено вплив проникності хвилелому на трансформацію хвилі. Передбачається, що вертикальний хвилелом, на відміну від абсолютно жорсткого, характеризується кінцевою проникністю і може поглинати енергію набігаючих хвиль. У зв'язку з цим досліджено поширення поверхневих гравітаційних хвиль у прямокутній системі координат. Наведено традиційні реалізовані приклади відбору енергії хвилі та їх математичний аналіз. Із закону збереження енергії при відбиванні від вертикальних стінок випливає залежність для коефіцієнта відбиття як функції коефіцієнта проникнення. Наведено результати експериментальних досліджень поширення поверхневих гравітаційних хвиль та їх взаємодії з поглинаючими стінками. Отримано залежності коефіцієнтів відбиття і проникнення хвилі, а також коефіцієнтів дисипації енергії хвилі в залежності від проникності вертикальної стінки, глибини потоку і довжини початкової хвилі. Наведено інтегральні та спектральні характеристики поля хвиль і коливань тиску на обтічній поверхні водопроникного хвилелому.

Ключові слова: трансформація хвиль, проникний хвилелом, чисельне та фізичне моделювання, відбиття та проникнення хвиль, дисипація хвильової енергії.

Introduction. Coastal regions play an important role in the economic development of many countries of the world. In these regions, construction and operation of a large number of hydraulic structures, berths, zones and recreation centers is carried out. The main problem for the development of these regions and coastal waters is the protection of coasts, harbors and maritime infrastructure. Means of protection should be highly effective, increased environmental safety and should be the most reliable and, if possible, cheap. There are many types of coastal defense structures. These are dams, groins, berms, breakwaters and artificial beaches, bays, harbors and others. Protective structures of active, passive or complex type of action fully or partially protect coastal structures and the coastal zone [1 – 3]. These structures are built in the form of solid, discontinuous and permeable walls, inclined dams and breakwaters, submersible, floating and structures protruding above the sea surface. Depending on the type of structure, its location in the sea area, the principle and mechanism of action, the wave field is partially or completely reflected from the structure, transforms and penetrates through it, reducing wave loads on the protected objects. Coastal protection structures affect the movement of bottom sediments, change the circulation of the coastal current and the ecological situation in the protected water area. Breakwaters and dams are the most widely used coastal protection structures. Breakwaters are installed parallel or perpendicular to the shore to ensure safe navigation in the harbor and protect the coastline from erosion. Dams are built along the coastline to protect the coastline, reduce coastline erosion and the impact of surges and waves on coastal infrastructure.

The effect of hydrodynamic pressure on the wall of the breakwater and oscillations of hydrostatic pressure lead to significant loads on the structure. These structures are made massive and strong with large capital investments to withstand such loads [4]. Environmental restrictions and the increasing cost of building of protection structures, such as vertical or inclined breakwaters, require consideration of alternative solutions to traditional full protection structures. To overcome the above problems, permeable breakwaters are used [5, 6]. Such breakwaters reduce the reflection of incoming waves relative to a solid vertical wall, provide partial passage of waves of an acceptable level into the protected area, and also allow the exchange of liquid between the open sea and the protected area. In addition, permeable walls allow marine fauna to move freely and form currents between piles that affect the movement of bottom sediments and pollution on the surface of the protected area. This significantly improves the ecology in the vicinity of permeable walls.

There are several points of view on the assessment of the interaction of waves with vertical solid and permeable breakwaters. One of them is the potential flow method, which is based on the calculation of the potential function for the corresponding boundary conditions [4, 7]. This method is based on the equations of conservation of energy, momentum and mass. In this theory, the wave load on the structure is determined by the maximum horizontal velocity of the fluid flow through the slots and pores of the structure with the high pressure gradient. Another method is based on the principle of head loss as fluid flows through the structure [8, 9]. Wave propagation and diffraction studies are presented in [10, 11]. The work [12] considers the selection of wave energy. The finiteness of the perturbation propagation velocity is studied in [10]. General methods for studying wave propagation and diffraction are given in [10]. The hydrodynamic characteristics of fully and semi-submerged vertical slotted breakwaters or walls have been theoretically and experimentally researched in works [13 – 15]. Horizontal permeable breakwaters have been studied in works [16, 17].

Wave reflection and transmission also dissipation of wave energy are the main hydrodynamic parameters of the efficiency of any breakwaters, including permeable breakwaters, which are used to protect sea coasts and coastal infrastructure. It should be noted that the breakwater works well when its ability to reflect waves and dissipate wave energy is high [18, 19]. In this case, the transfer of wave energy to the protected water area becomes minimal. Therefore, the study of the characteristics of reflection and transmission of waves, as well as the dissipation of wave energy in theoretical and experimental researches, are important and extremely relevant for understanding the effectiveness of breakwater structures [4, 10].

The purpose of the work is to study the features of the interaction of gravity waves with permeable breakwaters and to evaluate the effect of vertical slotted walls on the transformation of wave energy.

Formulation of the problem. The presence of a free surface ensures the application of an incompressible fluid model with good accuracy. Disturbances on the surface of the water propagate mainly due to the extrusion of the liquid, and not due to its dilatation (expansion-compression). Therefore, the vast majority of researches are based on potential theory.

Let us assume that the liquid, bounded by the free surface and the bottom, is oriented in a rectangular Cartesian coordinate system x, y, z, as shown in Fig. 1 for a section by a plane $y = 0$. It is assumed that the liquid is subject to the action of the mass forces of the gravitational field $\vec{F} = \rho g \vec{e}_z$, where ρ is the density of the liquid; g is the acceleration of gravity; $\vec{e}_z$ is the unit vector.

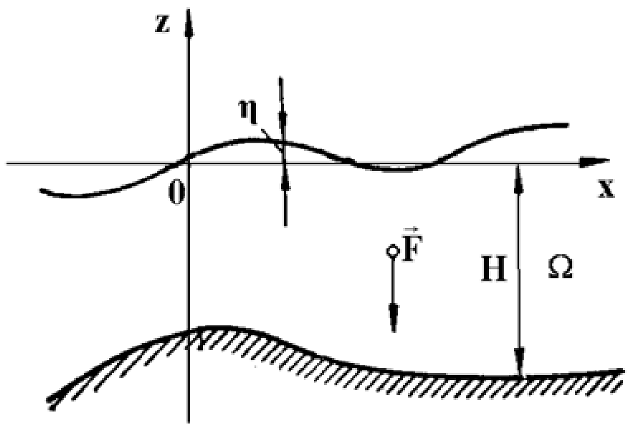

Fig. 1 – Geometry of the problem.

The free surface of a fluid at rest in an unperturbed equilibrium state occupies position $z = 0$, and the bottom surface is described by the equation $z = -H(x, y)$. The fluid can be unlimited, partially or completely limited in the direction of coordinates x, y. We will assume that the fluid is inviscid, incompressible, its motion is irrotational, and surface tension forces are not taken into account on the free surface. If waves arise on the surface of an initially at rest liquid, then they can be considered irrotational, neglecting the forces of viscosity, with a sufficient degree of accuracy. This follows from the Helmholtz theorem: the circulation along a closed curve is constant in time.

Under these assumptions, the wave motions of the fluid are described by the velocity potential $\varphi(x, y, z, t)$, which satisfies the Laplace equation

$$\nabla^2 \varphi = \frac{\partial^2 \varphi}{\partial x^2} + \frac{\partial^2 \varphi}{\partial y^2} + \frac{\partial^2 \varphi}{\partial z^2} = 0, \qquad \vec{v} = \vec{\nabla} \varphi \tag{1}$$

in the area Ω

$$x^s\left(y, t\right) \le x < \infty, \quad -\infty < y < \infty, \quad -H\left(x, y\right) \le z \le \eta\left(x, y, t\right).$$

The velocity potential must satisfy the following boundary conditions on the free surface:

– kinematic condition

$$\frac{\partial\varphi}{\partial x}\frac{\partial\eta}{\partial x}+\frac{\partial\varphi}{\partial y}\frac{\partial\eta}{\partial y}-\frac{\partial\varphi}{\partial z}+\frac{\partial\eta}{\partial t}=0, \tag{2}$$

– dynamic condition

$$g\eta+\frac{\partial\varphi}{\partial t}+\frac{1}{2}\left[\left(\frac{\partial\varphi}{\partial x}\right)^2+\left(\frac{\partial\varphi}{\partial y}\right)^2+\left(\frac{\partial\varphi}{\partial z}\right)^2\right]=F(x,\ y,\ t), \tag{3}$$

– bottom condition

$$\frac{\partial\varphi}{\partial x}\frac{\partial H}{\partial x}+\frac{\partial\varphi}{\partial y}\frac{\partial H}{\partial y}+\frac{\partial\varphi}{\partial z}=0, \tag{4}$$

– initial conditions

$$\begin{aligned}&\varphi(x,\ y,\ z,\ t)\big|_{t=0}=f_1(x,\ y,\ z),\\&\left.\frac{\varphi(x,\ y,\ z,\ t)}{\partial t}\right|_{t=0}=f_2(x,\ y,\ z).\end{aligned} \tag{5}$$

Here t is the time, $\eta(x,\ y,\ t)$ is deviation of the free surface, $\vec{v}$ is velocity vector, $\vec{\nabla}$ is gradient operator, $\vec{\nabla}=\vec{e}_x\frac{\partial}{\partial x}+\vec{e}_y\frac{\partial}{\partial y}+\vec{e}_z\frac{\partial}{\partial z}$, $x^s(y,\ t)$ is line of intersection of the free surface of the liquid with the shore, $F(x,\ y,\ t)$, $f_1(x,\ y,\ z)$ and $f_2(x,\ y,\ z)$ are given functions, $F(x,\ y,\ z)=0$ everywhere, except for the region Ω where surface perturbations are given.

The above statement (1) – (5) refers to the case when at the moment of time $t=0$ a disturbance is created on the surface of the liquid in the area D and it is required to determine the subsequent movement of the liquid, in particular, the shape of the free surface $z=\eta(x,\ y,\ t)$ and the components of the velocity vector must be determined.

Let us now assume that the components of the velocity vector $\vec{v}$, the deviation of the free surface η and the corresponding derivatives are small quantities, the squares and products which can be neglected compared to the linear terms. In this case, equations (2) and (3) are simplified and take the form

$$\frac{\partial\eta}{\partial t}-\frac{\partial\varphi}{\partial z}=0;\quad g\eta+\frac{\partial\varphi}{\partial t}=0\quad \text{at}\quad z=0. \tag{6}$$

If we exclude from these equations η, then we can obtain the condition

$$\frac{\partial\varphi}{\partial z}+\frac{1}{g}\frac{\partial^2\varphi}{\partial t^2}=0\quad \text{at}\quad z=0. \tag{7}$$

Solution of the specific problems within the framework of the above model (1) – (5) presents great difficulties. The above statement of the problem can only pretend to approximate correspondence to real wave processes.

Wave propagation in the shallow part is not considered, but approximations are applied that are based on the smallness of the ratio of the vertical scale, namely the depth $H=H_{\max}$ to the horizontal scale l (in the case of regular waves, this is the wavelength $l=\lambda$) [20].

The average energy flux per unit length of the wave crest that passes through a fixed vertical surface parallel to the crest is [21]

$$F_{\text{cp}}=\frac{1}{T}\int\limits_t^{t+T}\int\limits_{-d}^{\eta}\left(\rho\frac{V^2}{2}+p+\rho gz\right)u\,dz\,dt, \tag{8}$$

or taking into account the Bernoulli equation, in which it is assumed that the function $f(t)$ is included in $\partial\varphi/\partial t$, then from (8) we obtain

$$F_{\text{cp}}=-\rho\frac{1}{T}\int\limits_t^{t+T}\int\limits_{-d}^{\eta}\frac{\partial\varphi}{\partial t}\frac{\partial\varphi}{\partial x}dz\,dt. \tag{9}$$

This formula is suitable for any irrotational wave motion, which is either linear or non-linear. In the case of a linear periodic progressive wave, we have

$$\varphi=-a\frac{\omega}{k}\frac{\operatorname{ch}k(d+z)}{\operatorname{sh}kd}\cos(\omega t-kx). \tag{10}$$

Substituting (10) into (9) and neglecting some terms of higher orders, we obtain in the case of infinitely deep water

$$F_{\text{cp}}\big|_{d\to\infty}=\frac{1}{4}\rho g a^2\frac{gT}{2\pi},$$

and in the case of shallow water

$$F_{cp}\,|_{d\to 0} = \frac{1}{2}\rho g a^2 \sqrt{gd}\ .$$

From the above expressions and the expression for the wave energy, one can obtain the propagation velocity of the wave energy [22]

$$U_E = \frac{F_{cp}}{E_{cp}} = \frac{1}{2}c_p\left[1+\frac{2kd}{\operatorname{sh} 2kd}\right], \tag{11}$$

where c_p is the phase velocity. From (11) it follows that $U_E = \frac{c_p}{2}$ for infinitely deep water and $U_E = \sqrt{gd}$ for shallow water. This means that in deep water the energy propagates twice as slowly as the wave itself, and in shallow water at the velocity of the wave itself.

The energy of the incident wave field is equal to the sum of the energy of reflected waves and the energy of transmitted waves in accordance with the law of conservation of energy in the absence of absorption of wave energy by a vertical permeable wall. This is characterized by the reflection k_r and transmission k_t coefficients of the wave. The coefficient k_r is the ratio of the energy of the reflected wave to the energy of the incident wave, and the transmission coefficient k_t is the ratio of the energy of the transmitted wave to the energy of the incident wave. In this case, the wave transmission coefficient characterizes the resistance of the absorbent material. It follows from the law of conservation of energy that $\sqrt{k_r^2 + k_t^2} = 1$ under appropriate normalization.

Methods of experimental research. Experimental researches were carried out in a wave channel with a length of about 50 m, a width and a depth of 1 m. The water level in the channel varied from 0.5 m to 0.7 m. The channel was equipped with a shield generator of waves and an inclined wave absorber (at the end of the channel). Inside the channel, at a distance of about 40 m from the wave generator, permeable breakwaters were installed in the form of vertical slotted walls on a flat sandy base 0.2 m thick (Fig. 2, *a*). Thus, the water level at the location of the investigated breakwater varied from 0.3 m to 0.5 m. The side walls of the channel were made of glass for visual studies.

a

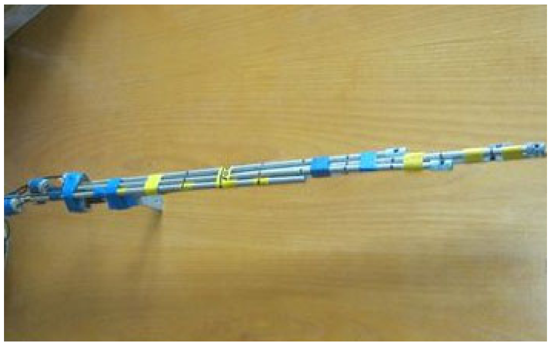

b

Fig. 2 – Experimental stand (a) and piezoresistive wave height sensors (b).

The experimental stand was equipped with control and measuring equipment, a system for processing and analyzing experimental data. Piezoresistive wave height sensors were installed along the longitudinal axis of the channel in front of the slotted wall and behind the wall (Fig. 2, *b*), and miniature piezoceramic pressure fluctuation sensors were located on the streamlined surface of the slotted wall. The pressure fluctuation sensors were installed flush with the streamlined surface of the slotted wall and recorded the wave pressure that acts on the breakwater as a result of the wave load. In addition, during the experiments, vibrations of the experimental setup and slotted walls were recorded using piezoceramic accelerometers.

Simultaneously 8 wave height sensors, among which traditional capacitive sensors were used, as well as specially designed and manufactured piezoresistive sensors [23, 24] were used in the experiments. Highly sensitive differential piezoresistive pressure sensors were vibrothermo compensated. In these sensors, sensitive elements based on microelectronic technology were applied to a thin quartz membrane, which bent under pressure, and the piezoresistive elements changed their resistance. Amplified electrical signals were fed to multichannel analog-to-digital converters. These sensors were installed in thin-walled tubes (Fig. 2, *b*), the lower ends of which were placed in water. Under the influence of wave motion, the water column in the tubes changed and caused pressure oscillations inside the tubes, which were recorded by piezoresistive sensors. The sensors had a resolution of up to 0.2 Pa or 0.02 mm of water column. These sensors recorded both static and dynamic pressure. Piezoresistive wave height sensors were calibrated by both absolute and relative methods.

The electrical signals of the wave height and pressure fluctuation sensors were amplified, filtered by appropriate equipment, and fed to 16-channel analog-to-digital converters, which were connected to computers or recorded on 4-

channel tape recorders. Processing and analysis of the experimental data were carried out on specialized one- and two-channel spectrum analyzers and personal computers. Universal and special algorithms and programs of probability theory and mathematical statistics [25] were used in the process of data processing and analysis.

The experiments were carried out with single-row slotted walls of different permeability, which were located inside the wave channel parallel to the front of regular waves (Fig. 3). Vertical cylinders with a diameter of 0.05 m, between which gaps were made, formed slotted walls. The permeability of such walls (the ratio of the area of the slots to the area of the wall) varied from 0 % (solid wall) to 60 %.

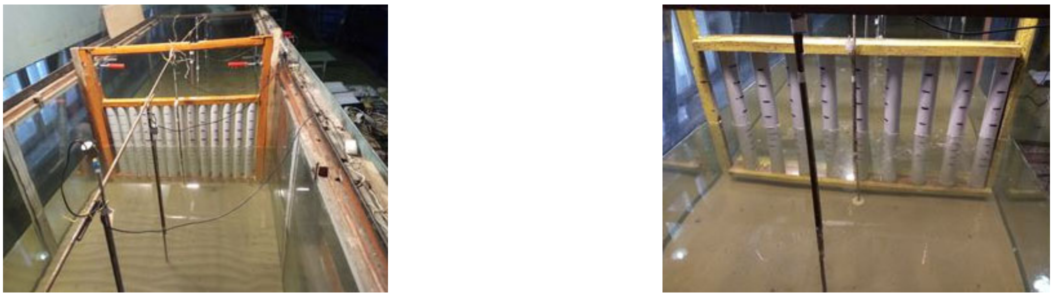

a *b*

Fig. 3 – Single-row cylindrical models of breakwaters with the permeability of 20 % (*a*) and 50 % (*b*) inside the wave channel.

The visualization of the wave motion and the features of the formation of jet and vortex flows between the cylinders of the slotted wall and in the vicinity of the wall itself was carried out using colored dyes and inks. The ink was introduced into the flow by means of miniature tubes and the ink movement trajectories were recorded by digital cameras and video cameras. Video and photographic material was sent to a specially created computer graphics station, where it was processed and analyzed using special programs [26 – 28].

Research results. The results of visual studies made it possible to evaluate the features of the wave motion, its interaction with permeable breakwaters, and to determine the spatio-temporal characteristics of the reciprocating motion of the fluid between cylinders of the slotted wall. So, Fig. 4 shows photographs of wave formation in the vicinity of slotted walls with a permeability of 20 % and 50 %.

a *b*

Fig. 4 – Wave heights in front of single-row slotted breakwaters and behind them with the permeability of 20 % (*a*) and the permeability of 50 % (*b*).

Studies have shown that an intense wave motion is formed in front of the slotted walls, depending on the modes of wave motion, the design and permeability of the breakwaters. It was found that behind the walls the height of the waves is much less than in front of them. The initial, reflected, standing and transmitted waves are observed on the wave surface in different time intervals. These waves interact with the permeable wall, generate wave pressures on the streamlined surface and alternating loads on the wall.

It is known that the efficiency of breakwaters or vertical walls, which are operated as coastal protection structures, is determined by the features of the formation of waves reflected and passing through the breakwater, as well as the ability to absorb or dissipate wave energy by the breakwater. The efficiency of such structures is determined by the coefficients of wave reflection (k_r), wave transmission (k_t) and wave energy dissipation (k_e). The determination of these coefficients in the research was carried out by measuring the wave heights in front of and behind the permeable breakwater.

The height of the reflected wave was determined by two methods. The first method is to determine the height of the reflected wave using two wave height sensors, one of which was at a wavelength distance (λ) from the breakwater, and the other at a distance of 1.25 λ from the breakwater. The first sensor measured the wave height (h_{an}) at the antinode of the standing wave, which is formed as a result of the interference of the incident wave and the reflected wave. The second sensor measured the wave height (h_n) at the node of the standing wave (Fig. 5, *a*).

The height of the incident wave was determined as

$$h_i = \frac{h_{an} + h_n}{2}\ , \tag{16}$$

and the height of the reflected wave was determined as

$$h_r = \frac{h_{an} - h_n}{2}\ . \tag{17}$$

Hence, the wave reflection coefficient was determined as

$$k_r = \frac{h_r}{h_i} = \frac{h_{an} - h_n}{h_{an} + h_n}\ . \tag{18}$$

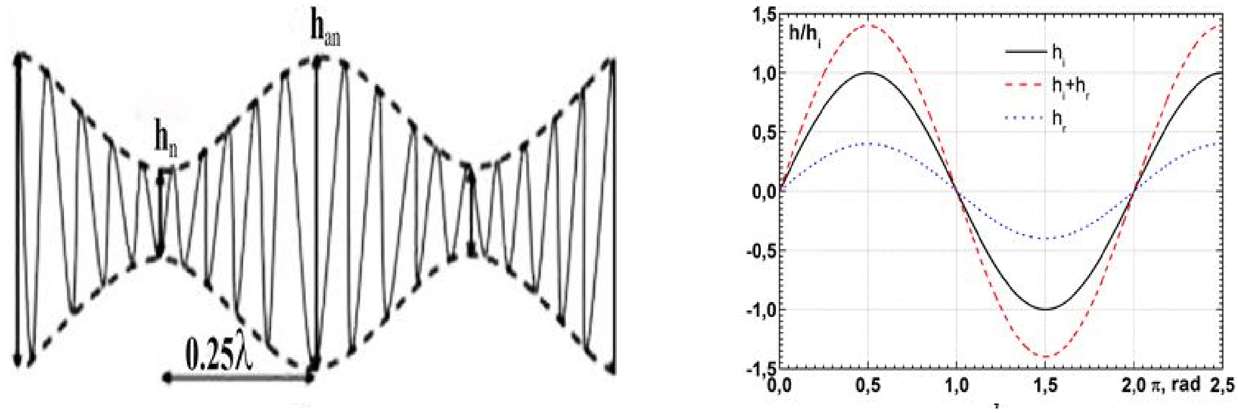

a *b*

Fig. 5 – Schemes for determining wave heights by the two-point method (*a*) and the one-point method (*b*).

Along with the two-point method, a one-point method was used to determine the height of the reflected wave from measuring the height of a standing wave by a wave height sensor, which was located along the axis of the wave channel in front of the breakwater at a distance of more than one length of the incident wave. At the same time, the height of the incident wave was measured in test studies of the operation of the wave generator in the absence of a breakwater inside the wave channel and the presence of wave absorption by wave absorbers. The height of the reflected wave was determined by subtracting the height of the incident wave from the height of the standing wave, as shown schematically in Fig. 5, *b*. Such a representation is possible when a standing wave is a superposition of the incident and reflection waves, which have the same period and transfer velocity (velocities are oppositely directed). As a result, the velocity of the standing wave in the longitudinal direction is zero and the standing wave performs only vertical oscillations. For this method of determining the reflected wave height, the wave reflection coefficient was determined as

$$k_r = \frac{h_r}{h_i}\ . \tag{19}$$

The wave reflection coefficients depending on the permeability of the slotted walls and relative depth are shown in Fig. 6.

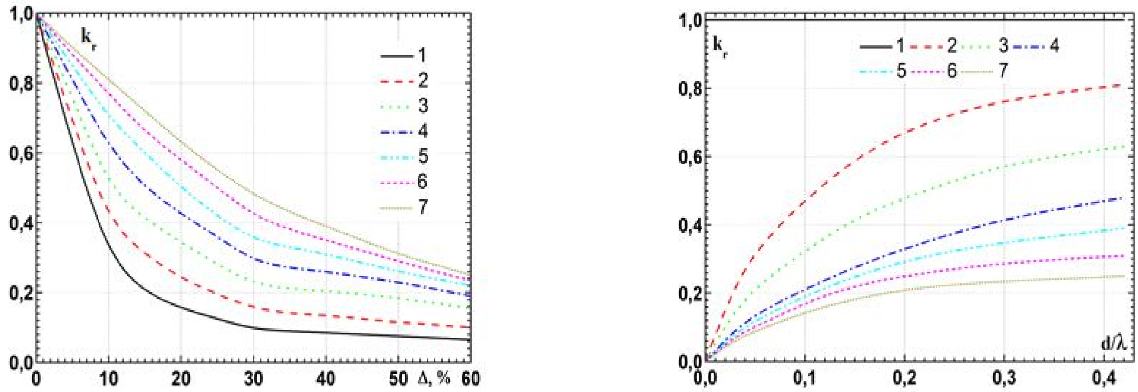

a *b*

Fig. 6 – Wave reflection coefficients depending on the permeability of the breakwater (*a*) and the depth (*b*).

Fig. 6, *a* shows the measurement results of the wave reflection coefficients depending on the permeability of the slotted wall for various depths, which are normalized by the wavelength (H/λ). Curve 1 was measured for relative depth $H/\lambda = 0.03$; curve 2 was measured for $H/\lambda = 0.06$; curve 3 – $H/\lambda = 0.11$; curve 4 – H/λ =0.16; curve 5 – $H/\lambda = 0.22$; curve 6 – $H/\lambda = 0.30$ and curve 7 – $H/\lambda = 0.42$. The research results show that with an increase in the permeability of the slotted wall, the wave reflection coefficients is monotonically decreased. In this case, the rate of decrease in the coefficients is higher for walls of low permeability. A solid breakwater completely reflects the original wave and the wave reflection coefficient for such a breakwater $k_r = 1$. As the dimensionless depth (H/λ) increases, the wave reflection coefficients increase, as shown in Fig. 7, *a*. At the same time, the rate of increase in the coefficient k_r is much higher for a slotted breakwater of low permeability than for a breakwater of high permeability.

The measurement results of the wave reflection coefficients by the vertical slotted wall depending on the relative depth for different breakwater permeability are shown in Fig. 6, *b*. Here, curve 1 was obtained for the solid wall with permeability $\Delta = 0$ %; curve 2 was measured for the wall with permeability $\Delta = 10$ %; curve 3 – for $\Delta = 20$ %; curve 4 – for $\Delta = 30$ %; curve 5 – for $\Delta = 40$ %; curve 6 – for $\Delta = 50$ % and curve 7 – for $\Delta = 60$ %. The research results show that the changes in the wave reflection coefficients have the opposite trend to those observed in Fig. 7, *a*. So, for shallow water conditions or very long waves, the wave reflection coefficient tends to zero. With increasing depth or decreasing wavelength, the coefficient k_r increases. The rate of increase of this coefficient is higher for the slotted walls of low permeability than for the walls with higher permeability. In deep water $H/\lambda > 0.3$, the heights of the reflected waves relative to the incident wave are higher than for the conditions of wave motion in shallow water. The waves are completely reflected from the breakwater for the solid wall $\Delta = 0$ % and the reflection coefficient takes the value $k_r = 1$ regardless of the depth or wavelength.

The transmitted wave height (h_t) was measured by wave height sensors behind the permeable breakwater at a distance greater than the incident wave length, and the wave transmission coefficient was determined as

$$k_t = \frac{h_t}{h_i}. \tag{20}$$

The wave transmission coefficients are shown in Fig. 7 depending on the permeability of slotted walls and relative depth. Fig. 7, *a* shows the results of measuring the wave transmission coefficients depending on the permeability of the slotted wall for various depths, which are normalized by the wavelength (H/λ). Curve 1 was measured for relative depth $H/\lambda = 0.03$; curve 2 was measured for $H/\lambda = 0.06$; curve 3 – $H/\lambda = 0.11$; curve 4 – $H/\lambda = 0.16$; curve 5 – $H/\lambda = 0.22$; curve 6 – $H/\lambda = 0.30$ and curve 7 – $H/\lambda = 0.42$. As the results of the study showed, the nature of the change in the wave transmission coefficient has the opposite trend with respect to the change in the wave reflection coefficient. It has been established that the wave transmission coefficient is increased with an increase in permeability and a decrease in depth or an increase in wavelength.

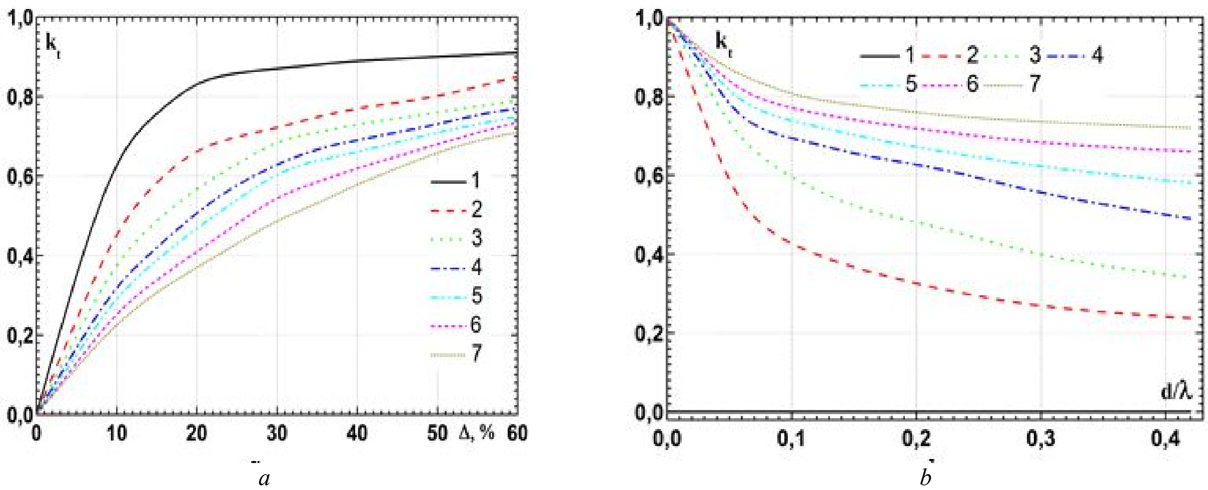

Fig. 7 – The wave propagation coefficients depending on the permeability of the breakwater (*a*) and the relative depth (*b*).

Changes of the wave transmission coefficient are shown in Fig. 7, *b* depending on the relative depth for different permeability of the slotted wall. Curve 1 was obtained for the solid wall with permeability $\Delta = 0$ %; curve 2 was measured for the wall with permeability $\Delta = 10$ %; curve 3 – $\Delta = 20$ %; curve 4 – $\Delta = 30$ %; curve 5 – $\Delta = 40$ %; curve 6 – $\Delta = 50$ % and curve 7 – $\Delta = 60$ %. The wave propagation coefficient is decreased with increasing relative depth and with increasing breakwater permeability. When the breakwater is a continuous vertical wall ($\Delta = 0$ %), then the wave does not transmit into the protected water area ($k_t = 0$).

The physical processes that occur during the interaction of waves with permeable protection structures have a big influence on the values of the reflection and propagation coefficients of the wave, as well as on the relationship between them. When a breakwater is installed in the marine environment, significant changes in the wave field occur. Interference, diffraction and transformation of waves are observed, reflected and transmitted waves are appeared, and wave breaking is occurred [17, 29]. The orbital velocities of wave motion are changed, turbulence is increased and horseshoe and wake vortices are generated in front of the breakwater and supporting piles, as well as jet streams are occurred between piles. This leads to an increase in friction between the surface of the breakwater and the moving liquid, as well as dissipation of wave energy.

The law of conservation of energy of the incident gravity wave, which interacts with a permeable breakwater, is expressed as follows:

$$E_i = E_r + E_t + E_d \,, \tag{21}$$

where E_i is the energy of the incident wave ($E_i = \rho g h_i^2 / 8$), E_r is the energy of the reflected wave ($E_r = \rho g h_r^2 / 8$), E_t is the energy of the transmitted wave through the breakwater ($E_t = \rho g h_t^2 / 8$), and E_d is the energy of the wave dissipation. Substituting into equation (21) the values E_r , E_t and E_d , as well as dividing the components of this equation by E_i , we obtain:

$$1 = (h_r / h_i)^2 + (h_t / h_i)^2 + E_d / E_i \tag{22}$$

or

$$k_e = 1 - (k_r^2 + k_t^2) \,. \tag{23}$$

The values of the wave dissipation coefficients depending on the permeability of the breakwater and the relative depth are shown in Fig. 8. Here, the numbers of the curves correspond to those shown in Fig. 6 and in Fig. 7.

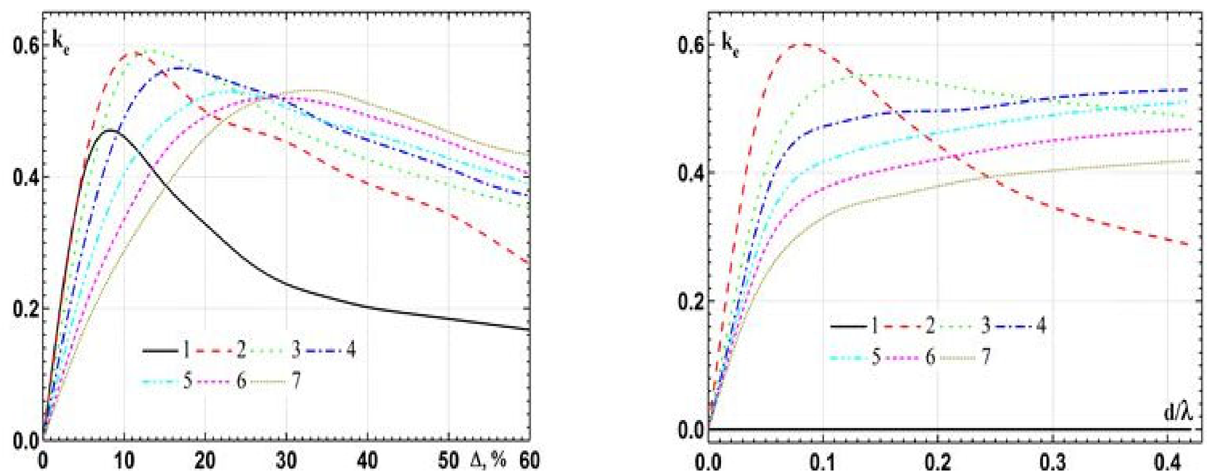

a *b*

Fig. 8 – The wave energy dissipation coefficients depending on the permeability of the breakwater (*a*) and the relative depth (*b*).

As the results of the study showed, the maximum wave energy dissipation was observed with the larger breakwater permeability when the relative depth was increased or when the wavelength was becoming shorter.

Conclusions. It has been established that vertical slotted walls, depending on the permeability, significantly affect the wave field, generate reflection waves and transmission waves, and also lead to significant wave energy dissipation. The dependences of the reflection and transmission coefficients of the wave, as well as the wave energy dissipation coefficient, depending on the permeability of the slotted breakwater and the relative depth of the water area are presented.

It was shown that the wave reflection coefficient was decreased with an increase in the breakwater permeability, and the wave transmission coefficient, on the contrary, was increased. The wave energy dissipation coefficient had a maximum value that was observed for greater permeability when the relative depth was increased compared to the wavelength. It was found that the wave reflection coefficient was increased with increasing relative depth, while the wave transmission coefficient, on the contrary, was decreased.

It has been established that the tonal components, which correspond to the fundamental frequency of the wave motion and its higher harmonics, prevail in the spectral power densities of the wave pressure fluctuations. In this case, these components were observed in front of the breakwater and behind it, as well as in the spectra of near-wall pressure fluctuations on the streamlined surface of the permeable breakwater.

Bibliography

1. *Sorensen R. M.* Basic coastal engineering. – NY : Springer Science, 2006. – 356 p.
2. *Khomytsky V. V.*, *Voskoboinick V. A.*, *Kharchenko A. G.*, *Voskoboinyk O. A.*, *Tereshchenko L. M.*, *Voskobiinyk A. V.*, *Nikitin I. A.* Beach protection by active shore protection structures // Ecological safety and nature management. – 2019. Vol. 32. – P. 60 – 77. DOI: 10.32347/2411-4049.2019.4.60-77.
3. *Voskoboinick V.*, *Khomitsky V.*, *Tereshchenko L.*, *Voskoboinick A.* Wave loads on protective dam of the Marine channel of the Danube-Black sea // Hydro-environment Research. – 2021. – Vol. 35. – P. 1 – 12. DOI: 10.1016/j.jher.2021.01.003.
4. *Choopanizade M. J.*, *Bakhtiari M.*, *Rostami M.* Wave transmission through the perforated half-depth block-made wall breakwater: An experimental study // Ocean Engineering. – 2020. – Vol. 215. – P. 107895. DOI: 10.1016/j.oceaneng.2020.107895.
5. *Alkhalidi M.*, *Alanjari N.*, *Neelamani S.* Wave interaction with single and twin vertical and sloped slotted walls // J. Mar. Sci. Eng. – 2020. – Vol. 8. – P. 589-1-23. DOI: 10.3390/jmse8080589.
6. *Koley S.*, *Panduranga K.* Energy balance relations for flow through thick porous structures // Int. J. Comp. Meth. Exp. Meas. – 2021. – Vol. 9. – P. 28 – 37. DOI: 10.2495/CMEM-V9-N1-28-37.
7. *Venkateswarlu V.*, *Karmakar D.* Numerical investigation on the wave dissipating performance due to multiple porous structures // ISH J. Hydraul. Eng. – 2019. – Vol. 3. – P. 314 – 324. DOI: 10.1080/09715010.2019.1615393.
8. *Lopez I.*, *Rosa-Santos P.*, *Moreira C.*, *Taveira-Pinto F.* RANS-VOF modelling of the hydraulic performance of the LOWREB caisson // J. Coastal Engineering. – 2018. – Vol. 140. – P. 161 – 174. DOI: 10.1016/j.coastaleng.2018.07.006.
9. *Qiao W.*, *Keh-Han W.*, *Wenqi D.*, *Yuqing S.* Analytical model of wave loads and motion responses for a floating breakwater system with attached dual porous side walls // J. Math. Prob. Eng. – 2018. – Vol. 14. – P. 1 – 14. DOI: 10.1155/2018/1295986.
10. *Selezov I. T*, *Kryvonos Yu. G.*, *Gandzha I. S.* Wave propagation and diffraction. Mathematical methods and applications – Singapore: Springer, 2018. – 241 p. DOI: https://doi.org/10.1007/978-981-10-4923-1.
11. *Andersen T. L.*, *Eldrup M. R.* Estimation of incident and reflected components in nonlinear regular waves over sloping foreshores // Coastal Engineering. – 2021. – Vol. 169. – P. 103974. DOI: https://doi.org/10.1016/j.coastaleng.2021.103974.
12. *Selezov I. T.*, *Savchenko S. A.* Propagation of surface gravitational waves and interaction with obstacles in the extraction of wave energy. – Kyiv: AVERS, 2014. – 214 p.
13. *Kriebel D. L.* Vertical wave barriers: wave transmission and wave forces // Proc. 23rd Coast. Engrg. Conf., ASCE. – 1992. – Vol. 2. – P. 1313 – 1326.
14. *Isaacson M.*, *Premasiri S.*, *Yang G.* Wave interactions with vertical slotted barrier // J. Waterway, Port, Coastal, Ocean Eng. – 1998. – Vol. 124. – P. 118 – 126. DOI: 10.1061/(ASCE)0733-950X(1998)124:3(118).
15. *Zhu D.* Hydrodynamic characteristics of a single-row pile breakwater // Coastal Engineering. – 2011. – Vol. 58. – P. 446 – 451. DOI: 10.1016/J. COASTALENG.2011.01.003.
16. *Krishnakumar C.*, *Sundar V.*, *Sannasiraj S. A.* Hydrodynamic performance of single- and double-wave screens // J. Waterway, Port, Coastal, Ocean Eng. – 2010. – Vol. 136. – P. 59 – 65. DOI: 10.1061/(ASCE)WW.1943-5460.0000025.
17. *Koraim A. S.* Hydraulic characteristics of pile-supported L-shaped bars used as a screen breakwater // Ocean Engineering. – 2014. – Vol. 83. – P. 36 – 51. DOI: 10.1016/j.oceaneng.2014.03.016.
18. *Poguluri S. K.*, *Cho I. H.* Analytical and numerical study of wave interaction with a vertical slotted barrier // Ships and Offshore Structures. – 2021. – Vol. 16. – P. 1012 – 1024. DOI: 10.1080/17445302.2020.1790299.
19. *Zhang C.*, *Li Y.*, *Zheng J.*, *Xie M.*, *Shi J.*, *Wang G.* Parametric modelling of nearshore wave reflection // Coastal Engineering. – 2021. – Vol. 169. – P. 103978. DOI: 10.1016/j.coastaleng.2021.103978.
20. *Whitham G. B.* Linear and nonlinear waves. – NY : John Wiley & Sons, 1999. – 638 p. DOI: 10.1002/9781118032954.
21. *Le Mehaute B.* An introduction to hydrodynamics and water waves. – NY: Springer-Verlag, 1976. – 323 p. DOI: 10.1007/978-3-642-85567-2.
22. *Stoker J. J.* Water Waves: The Mathematical Theory with Applications. – NY : John Wiley & Sons, 1992. – 567 p. DOI: 10.1002/ 9781118033159.
23. *Voskoboinick V.*, *Kornev N.*, *Turnow J.* Study of near wall coherent flow structures on dimpled surfaces using unsteady pressure measurements // Flow Turbulence Combust. – 2013. – Vol. 90. – P. 709 – 722. DOI: 10.1007/s10494-012-9433-9.
24. *Voskoboinick V. A.*, *Voskoboinick A. A.*, *Turick V. N.*, *Voskoboinick A. V.* Space and time characteristics of the velocity and pressure fields of the fluid flow inside a hemispherical dimple generator of vortices // J. Engineering Physics and Thermophysics. – 2020. – Vol. 93. – P. 1205 – 1220. DOI: 10.1007/s10891-020-02223-3.
25. *Bendat J. S., Piersol A. G.* Random Data: Analysis and Measurement Procedures, 4th Edition. – N.Y. : Willey, 2010. – 613 p. DOI: 10.1002/ 9781118032428.
26. *Voskoboinick V. A.*, *Voskoboinick A. V.*, *Areshkovych O. O.*, *Voskoboinyk O. A.* Pressure fluctuations on the scour surface before prismatic pier // Proc. 8th International Conference on Scour and Erosion (ICSE 2016) 12 – 15 September 2016 Oxford, UK. – 2016. – P. 905 – 910. DOI: 10.1201/9781315375045-115.
27. *Voskoboinick A.*, *Voskoboinick V.*, *Turick V.*, *Voskoboinyk O.*, *Cherny D.*, *Tereshchenko L.* Interaction of group of bridge piers on scour / Z. Hu, S. Petoukhov, I. Dychka, M. He (Eds.). Advances in Computer Science for Engineering and Education III. ICCSEEA 2020. // Advances in Intelligent Systems and Computing. – Springer, Cham, 2021. – Vol. 1247. – P. 3 – 17. DOI: 10.1007/978-3-030-55506-1_1.
28. *Voskoboinick V. A.*, *Gorban I. M.*, *Voskoboinick A. A.*, *Tereshchenko L. N.*, *Voskoboinick A. V.* Junction flow around cylinder group on flat plate / V. A. Sadovnichiy, M. Z. Zgurovsky (Eds.). // Contemporary Approaches and Methods in Fundamental Mathematics and Mechanics. – Understanding Complex Systems, Springer, Cham, 2021. – P. 35 – 50. DOI: 10.1007/978-3-030-50302-4_3.
29. *Reddy M. S.*, *Neelamani S.* Wave transmission and reflection characteristics of a partially immersed rigid vertical barrier // Ocean Engineering. – 1992. – Vol. 19. – P. 313 – 325. DOI: 10.1016/0029-8018(92)90032-Y.

References (transliterated)

1. Sorensen R. M. *Basic coastal engineering*. NY, Springer Science, 2006. 356 p.
2. Khomytsky V. V., Voskoboinick V. A., Kharchenko A. G., Voskoboinyk O. A., Tereshchenko L. M., Voskobiinyk A. V., Nikitin I. A. Beach protection by active shore protection structures. *Ecological safety and nature management*. 2019, Vol. 32, pp. 60–77. DOI: 10.32347/2411-4049.2019.4.60-77.
3. Voskoboinick V., Khomitsky V., Tereshchenko L., Voskoboinick A. Wave loads on protective dam of the Marine channel of the Danube-Black sea. *Hydro-environment Research*. 2021, Vol. 35, pp. 1–12. DOI: 10.1016/j.jher.2021.01.003.
4. Choopanizade M. J., Bakhtiari M., Rostami M. Wave transmission through the perforated half-depth block-made wall breakwater: An experimental study. *Ocean Engineering*. 2020., Vol. 215, P. 107895. DOI: 10.1016/j.oceaneng.2020.107895.
5. Alkhalidi M., Alanjari N., Neelamani S. Wave interaction with single and twin vertical and sloped slotted walls. *J. Mar. Sci. Eng*. 2020, Vol. 8, P. 589-1-23. DOI: 10.3390/jmse8080589.
6. Koley S., Panduranga K. Energy balance relations for flow through thick porous structures. *Int. J. Comp. Meth. Exp. Meas*. 2021, Vol. 9, pp. 28–37. DOI: 10.2495/CMEM-V9-N1-28-37.
7. Venkateswarlu V., Karmakar D. Numerical investigation on the wave dissipating performance due to multiple porous structures. *ISH J. Hydraul. Eng*. 2019, Vol. 3, pp. 314–324. DOI: 10.1080/09715010.2019.1615393.
8. Lopez I., Rosa-Santos P., Moreira C., Taveira-Pinto F. RANS-VOF modelling of the hydraulic performance of the LOWREB caisson. *J. Coastal Engineering*. 2018, Vol. 140, pp. 161–174. DOI: http://dx.doi.org/10.1016/j.coastaleng.2018.07.006.
9. Qiao W., Keh-Han W., Wenqi D., Yuqing S. Analytical model of wave loads and motion responses for a floating breakwater system with attached dual porous side walls. *J. Math. Prob. Eng*. 2018, Vol. 14, pp. 1–14. DOI: 10.1155/2018/1295986.
10. Selezov I. T, Kryvonos Yu. G., Gandzha I. S. *Wave propagation and diffraction*. *Mathematical methods and applications*. Singapore, Springer, 2018. 241 p. DOI: https://doi.org/10.1007/978-981-10-4923-1.
11. Andersen T. L., Eldrup M. R. Estimation of incident and reflected components in nonlinear regular waves over sloping foreshores. *Coastal Engineering*. 2021, Vol. 169, pp. 103974. DOI: https://doi.org/10.1016/j.coastaleng.2021.103974.
12. Selezov I. T., Savchenko S. A. *Propagation of surface gravitational waves and interaction with obstacles in the extraction of wave energy*. Kyiv, AVERS, 2014. 214 p.
13. Kriebel D. L. Vertical wave barriers: wave transmission and wave forces. *Proc. 23rd Coast. Engrg. Conf., ASCE*. 1992, Vol. 2, pp. 1313–1326.
14. Isaacson M., Premasiri S., Yang G. Wave interactions with vertical slotted barrier. *J. Waterway, Port, Coastal, Ocean Eng*. 1998, Vol. 124, pp. 118–126. DOI: 10.1061/(ASCE)0733-950X(1998)124:3(118).
15. Zhu D. Hydrodynamic characteristics of a single-row pile breakwater. *Coastal Engineering*. 2011, Vol. 58, pp. 446–451. DOI: 10.1016/J.COASTALENG.2011.01.003.
16. Krishnakumar C., Sundar V., Sannasiraj S. A. Hydrodynamic performance of single- and double-wave screens. *J. Waterway, Port, Coastal, Ocean Eng*. 2010, Vol. 136, pp. 59–65. DOI: 10.1061/(ASCE)WW.1943-5460.0000025.
17. Koraim A. S. Hydraulic characteristics of pile-supported L-shaped bars used as a screen breakwater. *Ocean Engineering*. 2014, Vol. 83, pp. 36–51. DOI: 10.1016/j.oceaneng.2014.03.016.
18. Poguluri S. K., Cho I. H. Analytical and numerical study of wave interaction with a vertical slotted barrier. *Ships and Offshore Structures*. 2021, Vol. 16, pp. 1012–1024. DOI: 10.1080/17445302.2020.1790299.
19. Zhang C., Li Y., Zheng J., Xie M., Shi J., Wang G. Parametric modelling of nearshore wave reflection. *Coastal Engineering*. 2021, Vol. 169, pp. 103978. DOI: 10.1016/j.coastaleng.2021.103978.
20. Whitham G. B. *Linear and nonlinear waves*. NY, John Wiley & Sons, 1999. 638 p. DOI: 10.1002/9781118032954.
21. Le Mehaute B. *An introduction to hydrodynamics and water waves*. NY, Springer-Verlag, 1976. 323 p. DOI: 10.1007/978-3-642-85567-2.
22. Stoker J. J. *Water Waves: The Mathematical Theory with Applications*. NY, John Wiley & Sons, 1992. 567 p. DOI: 10.1002/9781118033159.
23. Voskoboinick V., Kornev N., Turnow J. Study of near wall coherent flow structures on dimpled surfaces using unsteady pressure measurements. *Flow Turbulence Combust*. 2013, Vol. 90, pp. 709–722. DOI: 10.1007/s10494-012-9433-9.
24. Voskoboinick V. A., Voskoboinick A. A., Turick V. N., Voskoboinick A. V. Space and time characteristics of the velocity and pressure fields of the fluid flow inside a hemispherical dimple generator of vortices. *J. Engineering Physics and Thermophysics*. 2020, Vol. 93, pp. 1205–1220. DOI: 10.1007/s10891-020-02223-3.
25. Bendat J. S., Piersol A. G. *Random Data: Analysis and Measurement Procedures, 4th Edition*. N.Y., Willey, 2010. 613 p. DOI: 10.1002/978111 8032428.
26. Voskoboinick V. A., Voskoboinick A. V., Areshkovych O. O., Voskoboinyk O. A. Pressure fluctuations on the scour surface before prismatic pier. *Proc. 8th International Conference on Scour and Erosion (ICSE 2016) 12 – 15 September 2016*. Oxford, UK, 2016. pp. 905–910. DOI: 10.1201/9781315375045-115.
27. Voskoboinick A., Voskoboinick V., Turick V., Voskoboinyk O., Cherny D., Tereshchenko L. Interaction of group of bridge piers on scour. (Z. Hu, S. Petoukhov, I. Dychka, M. He (Eds.). Advances in Computer Science for Engineering and Education III. ICCSEEA 2020). *Advances in Intelligent Systems and Computing*. Springer, Cham, 2021, Vol. 1247, pp. 3–17. DOI: 10.1007/978-3-030-55506-1_1.
28. *Voskoboinick V. A., Gorban I. M., Voskoboinick A. A., Tereshchenko L. N., Voskoboinick A. V.* Junction flow around cylinder group on flat plate. (V. A. Sadovnichiy, M. Z. Zgurovsky (Eds.)). *Contemporary Approaches and Methods in Fundamental Mathematics and Mechanics*. Understanding Complex Systems, Springer, Cham, 2021. pp. 35–50. DOI: 10.1007/978-3-030-50302-4_3.
29. *Reddy M. S., Neelamani S.* Wave transmission and reflection characteristics of a partially immersed rigid vertical barrier. *Ocean Engineering*. 1992., Vol. 19, pp. 313–325. DOI: 10.1016/0029-8018(92)90032-Y.

Received (надійшла) 10.03.2025

Відомості про авторів / Information about authors

Воскобійник Володимир Анатолійович – доктор технічних наук, старший науковий співробітник, завідувач відділу гідродинаміки хвильових та руслових потоків, Інститут гідромеханіки НАН України, м. Київ; тел.: (+38044) 371-65-57; ORCID: http://orcid.org/0000-0003-2161-6923; e-mail: vlad.vsk@gmail.com.

Voskoboinick Volodymyr Anatoliyovych – Doctor of Technical Sciences, Associate Professor, Head of the Department of Hydrodynamics of Wave and Channel Flow, Institute of Hydromechanics of the National Academy of Sciences of Ukraine, Kyiv; tel.: (+38044) 371-65-57; ORCID: http://orcid.org/0000-0003-2161-6923; e-mail: vlad.vsk @gmail.com.

Воскобойник Олександр Анатолійович **–** кандидат технічних наук, старший науковий співробітник відділу гідродинаміки хвильових та руслових потоків, Інститут гідромеханіки НАН України, м. Київ; тел.: (+38044) 371-65-57; ORCID: http://orcid.org/0000-0001-8114-4433; e-mail: alexandr.vsk@gmail.com.

Voskoboinyk Oleksandr Anatoliyovych – Candidate of Technical Sciences, Senior Research Fellow at the Department of Hydrodynamics of Wave and Channel Flow, Institute of Hydromechanics of the National Academy of Sciences of Ukraine, Kyiv; tel.: (+38044) 371-65-57; ORCID: http://orcid.org/0000-0001-8114-4433; e-mail: alexandr.vsk@ gmail. com.

Воскобійник Андрій Володимирович – кандидат технічних наук, старший науковий співробітник, старший науковий співробітник відділу гідробіоніки та керування примежовим шаром, Інститут гідромеханіки НАН України, м. Київ; тел.: (+38044) 371-65-57; ORCID: https://orcid.org/0000-0001-8045-8625; e-mail: andrew.vsk@ gmail.com.

Voskobiinyk Andriy Volodymyrovych – Candidate of Technical Sciences, Associate Professor, Senior Research Fellow at the Department of Hydrobionics and Boundary Layer Control, Institute of Hydromechanics of the National Academy of Sciences of Ukraine, Kyiv; tel.: (+38044) 371-65-57; ORCID: https://orcid.org/0000-0001-8045-8625; e-mail: andrew.vsk@gmail.com.

Харченко Анатолій Григорович – головний інженер-електромеханік відділу гідродинаміки хвильових та руслових потоків, Інститут гідромеханіки НАН України, м. Київ; тел.: (+38044) 371-65-57; ORCID: http://orcid.org/0000-0002-5832-7714; e-mail: Anatoliy.kharchenko62@gmail.com.

Kharchenko Anatolii Grygorovych – chief electromechanical engineer of the Department of Hydrodynamics of Wave and Channel Flow, Institute of Hydromechanics of the National Academy of Sciences of Ukraine, Kyiv; tel.: (+38044) 371-65-57; ORCID: http://orcid.org/0000-0002-5832-7714; e-mail: Anatoliy.kharchenko62@gmail.com.

Труденко Денис Володимирович – аспірант кафедри мостів, тунелів та гідротехнічних споруд, Національний транспортний університет, м. Київ; тел.: (+38044) 280-79-78; ORCID: https://orcid.org/0009-0001-3720-1952; e-mail: tdv.83@ukr.net.

Trudenko Denys Volodymyrovych – PhD Student of the Department of Bridges, Tunnels and Hydrotechnical Structures, National Transport University, Kyiv; tel.: (+38044) 280-79-78; ORCID: https://orcid.org/0009-0001-3720-1952; e-mail: tdv.83@ukr.net.